

JAVA-Based Plugin for Tomographic Reconstruction in SPECT

M.A. Andrade, A. M. Marques da Silva, M.V. Silva da Costa, D. F. Guimarães de Azevedo, *Member, IEEE*

Abstract– The aim of this study was to develop a plugin for software ImageJ able to do tomographic reconstruction for SPECT. Two methods of tomographic reconstruction for emission images were implemented: Filtered Backprojection (FBP) and an Maximum Likelihood-Expectation Maximization (MLEM). Filters were also implemented. Validation tests were carried out with simulated images of geometric models and an anthropomorphic model through Monte Carlo method. The analysis of convergence of the iterative method through the estimate of the relationship between the average uptake and the standard deviation resulted in an indication of reconstruction with 10 to 15 iterations. The images reconstructed through the ML-EM method with attenuation correction presented better visual quality than the non-corrected images. For 128x128 pixel images, MLEM time is 33 times longer than FBP. When attenuation correction is carried out time increases 3.5x.

I. INTRODUCTION

Image reconstruction from projections forms the basis for SPECT. The projections are mathematically modified to Reconstruct the three-dimensional distribution of a Radiopharmaceutical accurately. Although many algorithms exist, the most used are filtered backprojection (FBP) and Maximum likelihood expectation maximization (MLEM). Tomographic reconstruction takes place on software according To the manufacturer of spect device, or proprietary software. Nowadays, proprietary software leads the market of Medical imaging for diagnostic purposes because most Equipment cannot be dissociated in hardware and software. Proprietary software is software with restrictions on using, Copying and modifying as enforced by the proprietor. Its Restrictions make it an antonym of free software and limit the User resources on tools for image processing. Moreover, it leads to too much dependency on future versions and upgrades With high costs [1].

Manuscript received November 23, 2007. This work was supported by FRIDA program (Fundo Regional para a Inovação Digital na América Latina e do Caribe) and CAPES (Coordenação de Aperfeiçoamento de Pessoal de Nível Superior).

M. A. Andrade, was with Pontifical University of Rio Grande do Sul, RS, Brazil. She is now with the Science and Techonology Department, State Government of Rio Grande do Sul, RS, Brazil (telephone: +55 51 3288-7484, e-mail: michele.alberton@gmail.com).

A. M. Marques da Silva is with the Department of Physics, Pontifical University of Rio Grande do Sul, Av Ipiranga 6681, Porto Alegre, RS, Brazil (telephone: +55 51 3320-3535, e-mail: ana.marques@pu.rs.br).

D. F. Guimarães de Azevedo, is with the Electrical Engineering Department, Pontifical University of Rio Grande do Sul, Av Ipiranga 6681, Porto Alegre, RS, Brazil (e-mail: dario@ieee.org).

M. V. Silva da Costa is with the Department of Physics, Pontifical University of Rio Grande do Sul, RS, Brazil (e-mail: costa.vinicius@gmail.com).

The IT market is one of the most promising, growing at a rate of 10% per year. The development of this sector become, in the last year, of vital importance from the point of view of technological independence. The decrease of foreign software dependence is a challenge for the rising of Brazilian software market

The development of free software tools and applications has been pointed as a possible way to minimize the effects of this situation. Software is considered free when it can be executed, copied, distributed, studied, or even modified and improved by the user. Other kind of software licensing is open source, wich allows the user only to see the systems source code. A free software is open source but the opposite is not true [2].

Tomographic reconstruction requires advanced image processing and viewing tools, wich are commonly sold together with image acquiring equipment. This model presents two considerable disadvantages. First is, as long as these tools are developed for use with specific equipments and purposes, many of the features are pre-programmed, not exploring a big amount of data available on the image. Second drawback is that these tools do not have open source code and so its potential cannot be explored, in case studies and in medical radiology research and education.

The objective of this work was to develop a plugin, named Nucmed, for tomographic reconstruction for SPECT using existing image-processing software imagej, which is widely esed by researchers because it's free, available on the web and extensible through plugins.

II. MATERIALS AND METHODS

A. ImageJ

Efficient implementation of core processes and permanently improvement of systems integration is important. Because of that, cross-platform open source software, appropriate for working with several types of images and extensible through plugins, was required. To make this happen, we have chosen software *ImageJ* [3]. ImageJ was designed with an open architecture that provides extensibility via Java plugins. It has the ability to apply lookup table, tools for zooming, resizing, rotating, contrast, regions of interest (ROIs) delimitation tools, histograms, plots of profiles and other measures, very useful for medical image processing. Moreover, user-written plugins make it possible to solve almost any image processing or analysis problem. One of the limitations of the software is its ability to deal with double data type since it supports only four data types (byte, short,

float, RGB). Furthermore, the addition of a set of open source Java packages – *Jsci* [4] – with unidimensional fourier transform methods and classes to handle complex numbers had been necessary.

We have implemented two methods of tomographic reconstruction for emission images: an analytical method (FBP) and an iterative method (MLEM). FBP method is the most widely used reconstruction method in clinical environment because its speed and relative ease of implementation. However, its susceptible to major artifacts, amplification of high frequency noise and do not take into account physical aspects of imaging system and data acquisition [5]. Ramp, Butterworth, Shepp-Logan and Hamming filters were implemented. Different filters (filter-window combinations) are obtained by multiplying the respective window by the ramp filter. Simple backprojection is also available. MLEM estimation is an attractive reconstruction method for SPECT, because of its ability to model Poisson noise, non-uniform attenuation, detector response and scatter [5].

All parameters (e.g., cut-off frequency, number of iterations) can/must be set through the user interface.

Fig. 1 presents an parcial Activity Diagram, in Unified Modeling Language (UML) notation, for ImageJ which includes the plugin developed in this work.

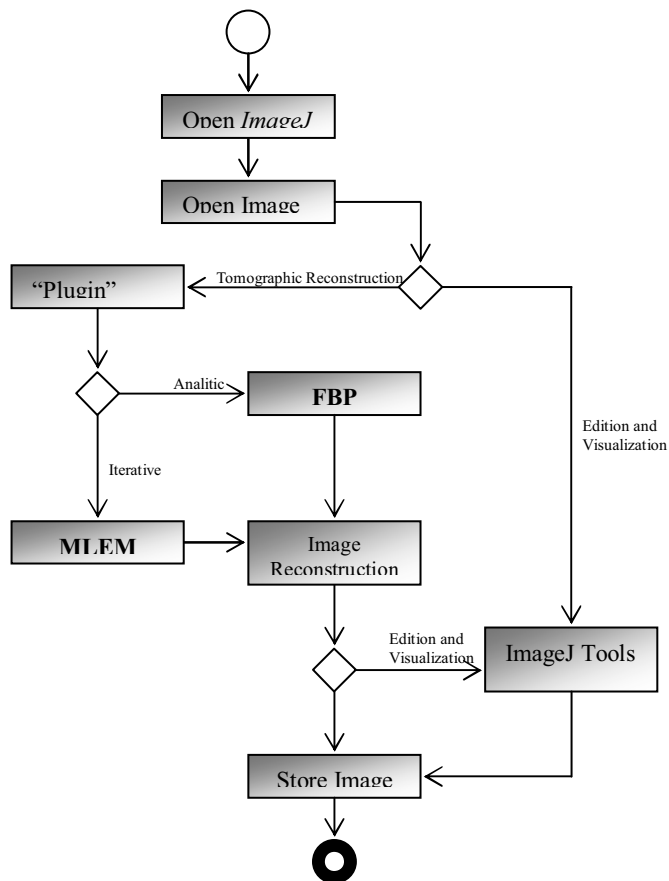


Fig. 1. Activity Diagram in UML notation describing the state of activities by showing the sequence of activities performed since ImageJ is started. Users

must open an image (sinogram) before selection of tomographic reconstruction method (FBP or MLEM) from menu “Plugins”. When tomographic reconstruction process is over, result is displayed and further edition and/or analysis can be done. Final image can be saved in any type of data supported by ImageJ.

B. Monte Carlo Simulation

Monte Carlo simulation is a technique that involves using random numbers and probability to solve problems. It has been an sophisticated tool to model systems which real data are difficult or expensive to reproduce, complex system which cannot be described by equations that leads to an direct analytical solution or to validate mathematical models and compare them with real experiments.

Validation tests were carried out with simulated images of geometric models and anthropomorphic model through Monte Carlo method. Projection data were generated using SimSet simulator [7]. The simulations were performed for ^{99m}Tc , parallel LEHR collimator, energy window of 20% centered at 140 keV.



Fig. 2. Geometrical Models. On the left, cylinder filled with water and activity of $50 \mu\text{Ci}/\text{cm}^3$. On the left, punctual source filled with water and activity of $30 \mu\text{Ci}/\text{cm}^3$ (not centered).

For both models in Fig. 2 we simulated 120 projections over 360° . Matrix size was 64×64 and pixel size 0.625 cm .



Fig. 3. White area corresponds to the heart activity ($50 \mu\text{Ci}/\text{cm}^3$) and blue area corresponds to the body activity ($10 \mu\text{Ci}/\text{cm}^3$). Big black circles represent lungs and small black circle the spine. There is no activity in these areas.

The geometric model in Fig. 3 represents torso structures (heart, lung, spine) using circles and ellipses. We simulated 128 projections over 360° . Matrix size was 128×128 and pixel size was 0.312 cm . We used this model for contrast measurements because it has good delimitations on hot and cold areas.

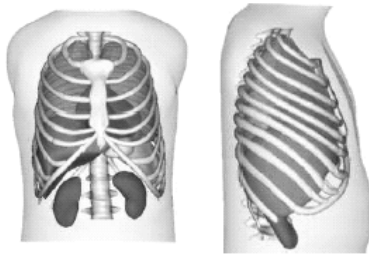


Fig. 4. Frontal and lateral view of NCAT 4D [6] phantom is an anthropomorphical model that was built with segmented images from the project *Visible Human CT*.

In this work we added respiratory and cardiac movement to phantom NCAT 4D described in Fig. 4. We simulated 128 projections over 360°. Matrix Size was 128x128 pixels and pixel size 0.3125 cm.

C. Data Analysis

To investigate the quality of reconstructed images, we considered the parameters above:

1. Image profiles through reconstructed images
2. Normalized Mean
3. Normalized Standard Deviation

$$NSD = \frac{1}{\lambda} \sqrt{\frac{\sum_{j=1}^N (\lambda_j - \bar{\lambda})^2}{N-1}} \quad (1)$$

4. Contrast

$$C = \frac{|M_L - M_F|}{M_L + M_F} \quad (2)$$

Where M_L is mean activity in a cold or hot spot and M_F is mean activity of the neighbor region with constant background activity.

III. RESULTS

A. Features

Common features of the NucMed reconstruction methods are: (i) GUIs to set parameters; (ii) inherit class *PlugIn* from ImageJ, which allows the plugin to be called from the Menu *Plugins*; (iii) input data must be a sinogram; (iv) support grayscale and RGB images; (v) support stacks.

Fig. 5 presents the NucMed plugin interface. NucMed plugin windows are called from ImageJ main interface through menu *Plugins*. Parameters must be set before reconstructing images.

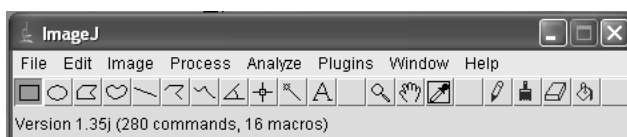


Fig. 5. NucMed plugin interface. ImageJ main interface (top), sinogram (left), FBP window (center). MLEM window (right).

Since you can work with many images at the same time, for MLEM reconstruction, when carrying out attenuation correction, it's important to inform on the dialog box which image corresponds to the sinogram and the attenuation map.

Estimated times for reconstructing 32 bit/pixel images on Pentium 4 platform with 2.80GHz and 512 MB RAM are shown in Table I.

TABLE I
ESTIMATED TIME, IN SECONDS, FOR IMAGE (32 BIT/PIXEL) RECONSTRUCTION.

	64x64	128x128	256x256
FBP Ramp and Butterworth, wc=0.27, N=9	0.109	0.640	1,966
MLEM without attenuation correction	5.226	21.14	169.93
MLEM with attenuation correction	19.51	71.80	538.52

We can see that FBP is much faster than MLEM. When attenuation correction is applied, time for reconstruction increases 3.5 times.

B. Implementation

In this section we present a few lines of source code written for this plugin.

```

1 public class FBP_ extends javax.swing.JFrame implements ij.plugin.PlugIn {
2
3     public static ImagePlus imp;
4     ...
5     public void run(String str) {
6         if( str.equals( "about" ) )
7             IJ.showMessage("\n"+ " Desenvolvido por NIMed -
8                 PUCRS - Brasil\n"+
9                 "\n Homepage http://www.pucrs.br/fisica/nucmed ");
10        else {
11            imp = IJ.getImage();
12            tamanho_imagem = imp.getWidth();
13            type = imp.getType();
14            if((tamanho_imagem> 0) &&
15                (Funcoes.isPowerOf2(tamanho_imagem))) {
16                IJ.register(FBP_.class);

```

```

17     setVisible(true);
18     }
19     else {
20     IJ.showMessage(Funcoes.MENSAGEM_
21     IMAGEM_NAO_COMPATIVEL);
22     }
23     }
...
}

```

Above is described *FBP_* class which inherits *javax.swing.JFrame* and implements the interface *ij.Plugin.PlugIn* (line 1). This part allows creation of user friendly interface (graphical) and connects the source code of NucMed plugin to ImageJ. It's important to keep *_* (underscore) together with class name, otherwise it won't appear in menu Plugins in ImageJ. At line 3 we declare a *ImagePlus* type variable called *imp* which stores the content of image (sinogram) selected by user and visible on screen, as we can see at line 10, through the method *getImage()*. Image size must be tested, as we can see at line 15 through method *isPowerOf2()*, to avoid errors when calculating Fourier transform.

NucMed plugin works with 8, 16 and 32 bit/pixel, grayscale or RGB images. Also accepts stacks. Parameters are set at specif windows according to chosen reconstruction method.

C. Validation Tests

We used the punctual source to verify total counts. Fig. 6 shows 3D representation of punctual source images reconstructed with simple backprojection and MLEM. Simple backprojection shows high intensity background and higger blurring.

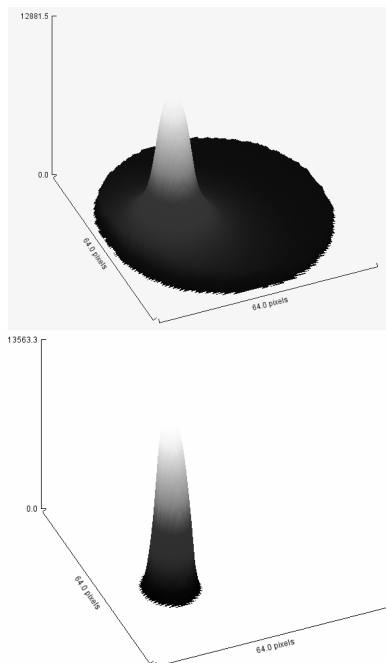


Fig. 6. 3D representations of punctual source reconstructed with (top) simple backprojection and (bottom) MLEM, 10 iterations, no attenuation correction. Simple backprojection shows high intensity background and higger blurring.

To identify the best number of iterations for MLEM algorithm, we observed the reconstructed images from the cylindrical model. Calculations of normalized mean and normalized standard deviation in a circular ROI with a diameter of 6 pixels in an uniform area of the image.

Fig. 7 presents the normalized mean and normalized standard deviation as a function of iteration number in the cylindrical phantom using MLEM. The MLEM algorithm reached convergence in 10 iterations.

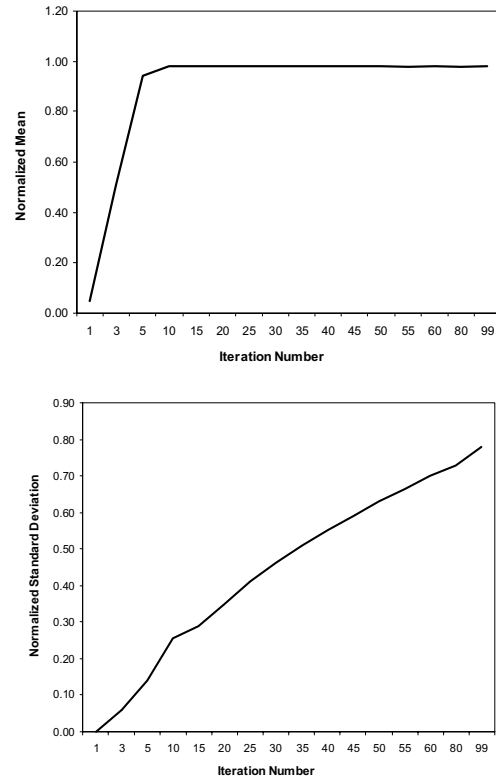


Fig. 7. Normalized Mean (top) and Normalized Standard Deviation (NSD) (bottom) in the cylindrical phantom.

From the 10th iteration there's is no significant change in mean pixels value from the region of interest and Standard deviation indicates that noise increases. Then we suggest 10 to 15 iterations when reconstructing images with MLEM.

The attenuation correction effect is shown in Fig. 8. The attenuation correction improves image uniformity.

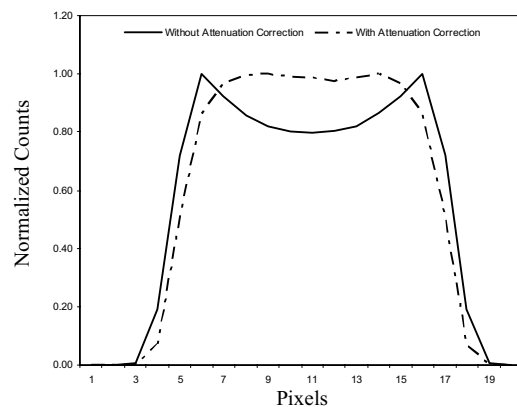


Fig. 8. MLEM reconstruction profiles with and without attenuation correction using projection-backprojection.

By applying attenuation correction one can see that the uptakes in the center of the cylinder are recovered, providing better uniformity. That can also be checked in Fig. 9.

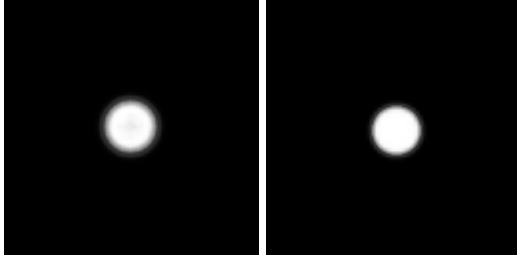


Fig. 9. Cylindrical model images reconstructed with MLEM, 10 iterations. On the left without attenuation correction. On the right with attenuation correction. Uniformity is improved when applying attenuation correction methods.

Different filters were implemented and their applications for FBP are given in Fig. 10. Cut-off frequency 0.50 cycles/pixel was set for Ramp, Hamming and Shepp-Logan filter; for Butterworth 0.27 cycles/pixel and order $N = 9$.

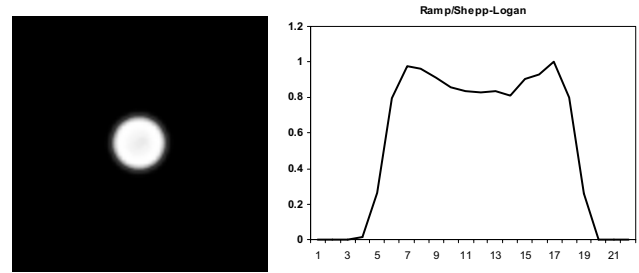


Fig. 10. Profiles of FBP reconstructions with Ramp, Ramp/Butterworth, Ramp/Hamming, and Ramp/Shepp-Logan filters. Since FBP does not take into account attenuation correction methods, uptakes from the central region become underestimated.

We calculated contrast of images reconstructed with FBP and MLEM without attenuation correction of the geometric model of torso. This model presents hot and cold (high and low activity) regions (heart and lung) and intermediate activity region (body).

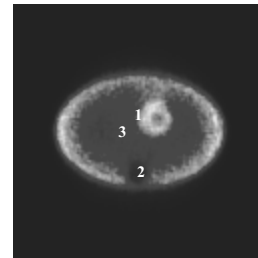


Fig. 11. Reconstructed image from geometric model of torso. Numbers represent hot region (1), cold region (2) and background (3). Each region corresponds to a circular ROI with a diameter of 6 pixels.

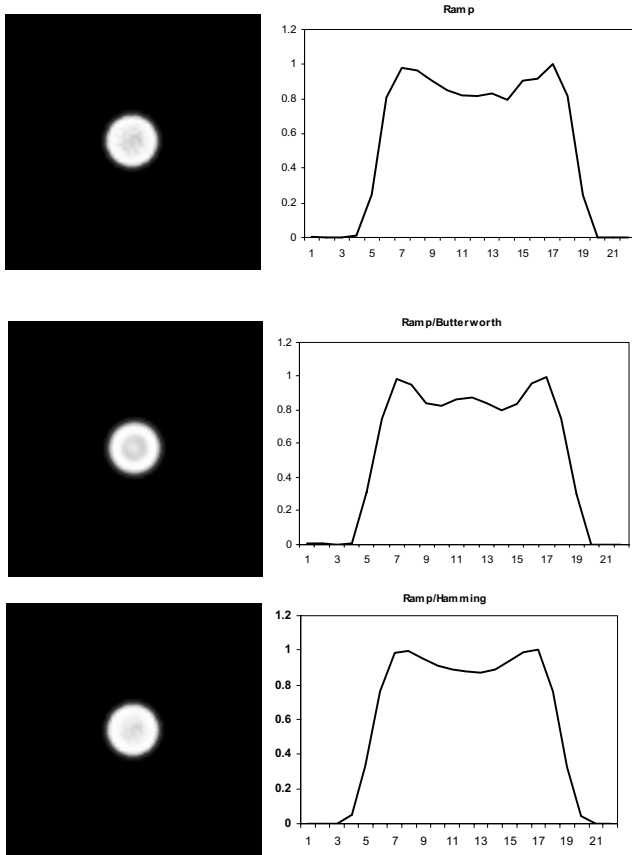
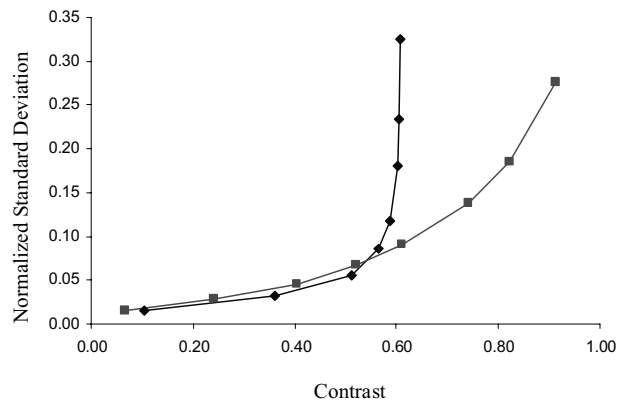


Fig. 12 shows that contrast quickly increases until 20th iteration for the hot area. Contrast values varies 4% from 20th to 60th while standard deviation grows.



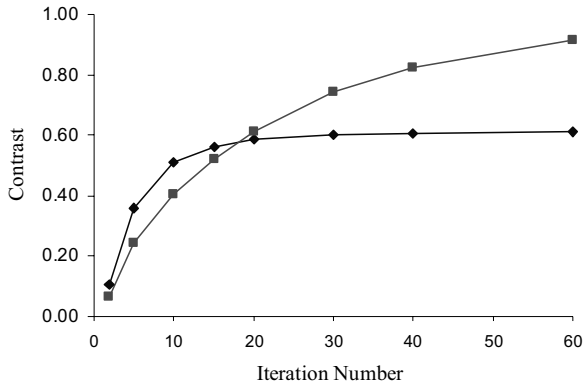


Fig. 12. Relationship between contrast, iteration number and normalized standard deviation for MLEM. ◆ Indicates hot areas and ■ indicates cold areas.

Contrast values for images reconstructed with FBP are presented in Fig. 13.

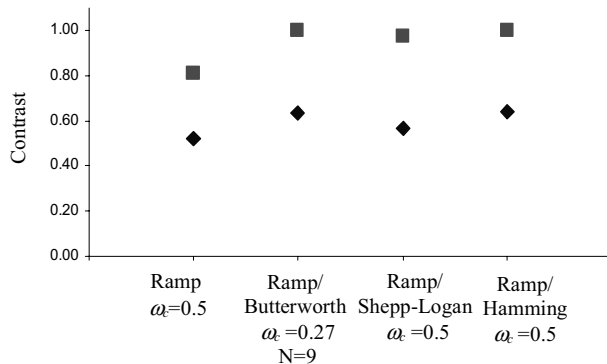


Fig. 13. Contrast values for FBP with different filter/window combinations. Cold areas presented high contrast than hot areas. ◆ Indicates hot areas and ■ indicates cold areas.

All combinations showed that in cold areas contrast values are higher.

Fig. 14 shows images obtained with the FBP and MLEM algorithms.

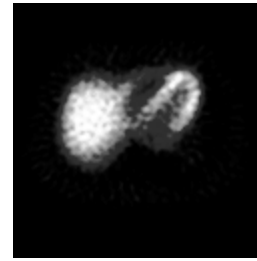
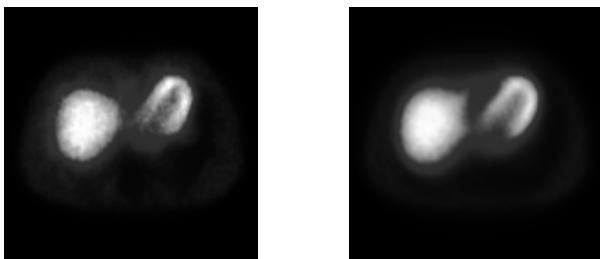


Fig. 14. Reconstructed images of anthropomorphic phantom. MLEM with and without attenuation correction (top). FBP with Ramp/Butterworth filter (bottom).

IV. DISCUSSION

The system ImageJ is quite stable and appears to be immune to user errors due to its easy-to-use operationability. Besides, is professional level image-processing software, is freely available on the Web and its constantly evolving.

The goal of developing a plugin for ImageJ was to reduce dependency on proprietary software and provide opportunity to develop general studies independent of platform or manufacturer.

V. CONCLUSIONS

In this work a plugin for tomographic reconstruction in SPECT was implemented based on open-source freely available software ImageJ (www.pucrs.br/fisica/nucmed). Simulated SPECT projections were generated using SimSet simulator for validation tests on reconstructed images. Results from tests with FBP algorithm showed similar results to MLEM if no attenuation correction is applied. However, images reconstructed with FBP appear to be noisier. FBP takes less time than MLEM to reconstruct images and if attenuation correction is taken into account, time can be 3.5 times longer. Further implementations need to be done to provide other tomographic reconstruction algorithms and improve quantification of the images.

VI. REFERENCES

- [1] S. Cherry, J. Sorenson, M. Phelps, "M. Physics in Nuclear Medicine", pp. 2003-523.
- [2] ComCiência Revista Eletrônica de Jornalismo Científico. 2004. Mercado de Software cresce na Periferia. Available on: <http://www.comciencia.br/200406/reportagens/03.shtml>.
- [3] Rasband, W.S., ImageJ, U. S. National Institutes of Health, Bethesda, Maryland, USA, <http://rsb.info.nih.gov/ij/>, 1997-2007.
- [4] Sourceforce Project. JSci web site. Available on: <http://jsci.sourceforge.net/>.
- [5] R. M Lewitt, S. Matej, "Overview of methods for image reconstruction from projections in emission computed tomography", Proceedings of the IEEE, Alemanha, v. 91, n. 10, pp. 1588-1611, oct. 2003.
- [6] University of Washington. SimSet User Guide. Available on: <http://depts.washington.edu/>.
- [7] W. P. Seagars, "Development and Application of the new dynamic nurbs-based cardiad-torso (NCAT) phantom", Chapel Hill, 2001. 220 f. Doctoral Thesis – Department of Biomedical Engineering, University of North Carolina.